

Waveguide Filter Modeling and Simulation using Mode-matching, Fullwave Network Analysis and Swarm Optimization

I. Bouchachi^{1,2}, J. Mateu³, and M. L. Riabi¹

¹Laboratory of Electromagnetism and Telecommunications
University Mentouri of Constantine, Algeria
i.bouchachi@crti.dz, ml.riabi@yahoo.fr

²Research Center in Industrial Technologies CRTI, Algiers, Algeria

³Centre Technologic de Telecomunicacions de Catalunya (CTTC), Barcelona, Spain
jordi.mateu@cttc.cat

Abstract — This paper presents the modeling of waveguide bandpass filter synthesis. It consists of a combination of the most appropriate and reliable methods and techniques of analysis, simulation and optimization used in determined order and leading to a fast and accurate method of filter synthesis. An example of a forth-order filter synthesis is given, employing a symmetric configuration and symmetric response. The obtained results, reference measurement and commercial software simulator results are compared for validation.

I. INTRODUCTION

During the last two decades, there has been an extension and trivialization of passive microwave components. On one hand, this is due to the fact that an exponential rate of ICT users has stimulated more and more labs to focus their research on this field. On the other hand, the IT development of both sides, hard and soft, allowing a high-speed implementation of programs and softwares of synthesis, simulation and optimization.

Among these microwave components, we find filters and precisely the waveguide filters. After a first appearance in telecommunications few years before World War II [1], they still occupy an important role, because when it comes to design filters operating at microwaves with very high gains and conveying great power, the use of waveguides becomes inevitable.

The majority of filters are synthesized from an equivalent circuit or a coupling matrix [2]. By translating the circuits or matrices into a combination of inverters and resonators to create a filter, one can summarize the synthesis of a filter in 4 stages: first, the synthesis of the equivalent circuit or coupling matrix, the choice of the technology to use and computation of the initial dimensions of the filter, the simulation of the filter response, and optimization of its dimensions. Each step mentioned is in itself a vast field of research.

Over the years, different forms and filter topologies have been proposed. First, linear uniaxial filters, often Chebyshev or Butterworth [3] of a quite large size and a frequency response without transmission zeroes, Rhodes proposed bended structures to reduce the size of the filters [4]. Then, a big step was taken with dual mode filters proposed by Atia and Williams [5], where they assumed that each resonator of the filter can be coupled with all the others with a coupling factor M , allowing a reduction in the size of the filter and improving its frequency response. Later, a multitude of topologies (folded, box, cul-de-sac ...) were used [6-8].

Simultaneously, studies were conducted to study the behavior of electromagnetic fields through cavities and obstacles, either by treating the waveguides as a simple transmission line [9], or by a full-wave analysis that has been developed in order to take into account higher order modes. We can mention the method of moments [10], the spectral analysis [11] and mode matching [12], which offer high strength and reliability. Other numerical methods were used as the method of finite elements and finite differences [11], taking advantage of advances in computer science; these methods have been at the basis of several commercial software for microwave structures simulation, like Ansoft HFSS or CST STUDIO SUITE.

After several unsuccessful attempts to direct synthesis of waveguide filter without going through the optimization step, the latter has been proved essential. Often metaheuristic, iterative and inspired from nature like Genetic Algorithm, Practical Swarm Optimization and Neural Network, these optimization methods allow us to improve the filter response to satisfy predetermined filter specifications.

In this work, we have followed a method that we have found the most appropriate and reliable for the synthesis of a waveguide band-pass filter. It consists of

generating the coupling matrix starting from the desired response, drawing the global form from the filter topology and calculates the initial dimensions of the filter by the equivalent impedance image method [3]. After segmentation of the structure into several basic elements (junctions, bends and T-junction), each element is separately analyzed using the mode-matching technique, then the structure is treated as a network of these basic elements. In the end, we used PSO as an optimization method [13].

II. THE COUPLING MATRIX

In the early 1970s, Atia and Williams introduced the concept of the coupling matrix as applied to dual-mode waveguide filters [2]. This matrix describes the coupling between adjacent cavities, but also the coupling of each cavity with all other cavities of the filter. It is synthesized from the filter transfer function, the latter is itself obtained from the specifications of the filter response.

If in a filter, each resonator is coupled to all the others, the coupling matrix will contain only non-zero values. It is practically difficult and even impossible to achieve with a waveguide filter of higher order. Therefore, the goal is to use mathematical techniques to reduce the number of non-zero elements, leading to M matrices, similar to the initial matrix and which are substantially converted into filter.

In its final form, the matrix M proposed by Atia and Williams had symmetrical and multidagonal elements. This form is called the canonical form and it was the basic element of many researchers whose purpose was to propose other forms of coupling matrices. Several matrices have been obtained and successfully tested. They are called "topologies" [6].

Later, commercial software called CMS Filter & Coupling Matrix Synthesis Software is developed by Guided Wave Technology's. By simply introducing the characteristics of the filter and checking the box where we need to introduce a coupling, then the coupling matrix is calculated with high accuracy.

In this work, for the synthesis of a forth-order filter, having a symmetric frequency response of elliptical shape with four poles and two zeros of transmission located at (normalized frequency) -1.8 and 1.8 with 20 dB of return losses, a coupling matrix has been synthesized. It is presented as following:

$$M = \begin{bmatrix} 0 & 0.856 & 0 & -0.220 \\ 0.856 & 0 & 0.786 & 0 \\ 0 & 0.786 & 0 & 0.856 \\ -0.220 & 0 & 0.856 & 0 \end{bmatrix}, \quad (1)$$

with normalized input/output resistances $R=1.021$.

III. INITIAL DIMENSIONS

Once the coupling matrix obtained, the equivalent

electric circuit may easily be inferred, as replacing simply the coupling coefficient K_n by frequency invariant reactance inverters and the resonators by a capacitors C.

Figure 1 shows the equivalent circuit of a 4th order prototype filter, under the canonical form.

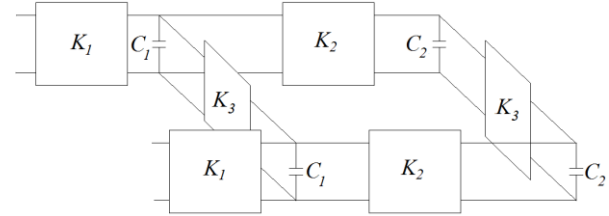


Fig. 1. Equivalent circuit of 4th order filter.

Since the final circuit consists of a quadripoles network connected in series and/or parallel, we can use ABCD to [Y] and [Y] to ABCD transformations to calculate the overall scattering parameters S_{11} and S_{21} ; they will give us the ideal frequency response of the filter. This latter will be our reference for the synthesis of the waveguide filter.

Figure 2 shows the response of the equivalent circuit after transforming the low-pass prototype into a bandpass filter, with 10 GHz as central frequency, a bandwidth of 300 MHz and 20 dB of return loss level.

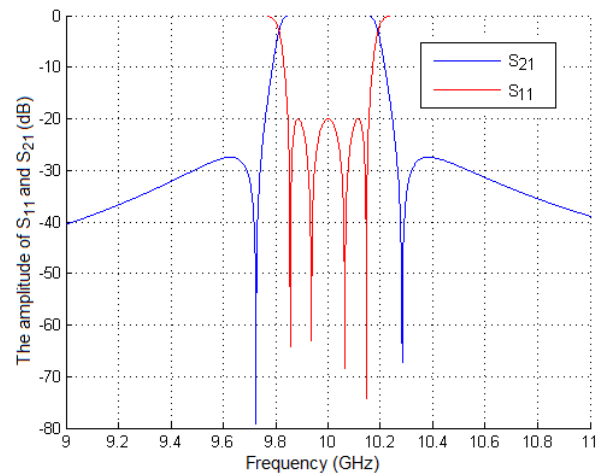


Fig. 2. S-parameters obtained from the coupling matrix.

The next step is to convert the equivalent circuit in a waveguide filter. To achieve this, we used the method of impedance images (impedance seen looking into a port of a network), which consists of inserting inside the waveguide geometric shapes or obstacles in order to obtain a structure having a similar impedance image than those quadripoles (inverter), these obstacles will separate a half-wave or quarter-wave cavities, which

will have the role of the resonators. To simplify the construction of the filter, in this work we have among our objectives to use as inverter only purely inductive or purely capacitive irises. The initial openings of these irises are deduced from curves drawn in [14] and the total electrical length θ of resonator cavity R is given by:

$$\theta_R = n\pi + \frac{1}{2} \left(\cot^{-1} \frac{B_1}{2} + \cot^{-1} \frac{B_2}{2} \right), \quad (2)$$

where B_1 and B_2 are the coupling susceptances of the two irises that define the cavity.

IV. MODE MATCHING METHOD

The mode-matching is a powerful method for analyzing waveguides with varying cross-section. It is based on the matching of the total mode fields at each junction between uniform sections (Fig. 3). The amplitudes of the modes at the output of a junction can be deduced in terms of the amplitudes of the mode spectrum at the input to the junction [12].

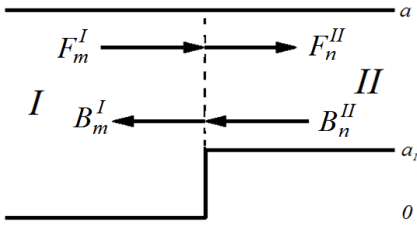


Fig. 3. Waveguide discontinuity.

Matching the transverse field components at the discontinuity we have:

$$\begin{cases} E_y^I = 0 & \text{if } : 0 \leq x \leq a_1 \\ E_y^I = E_y^{II} & \text{if } : a_1 \leq x \leq a \\ H_x^I = H_x^{II} & \text{if } : a_1 < x \leq a. \end{cases}, \quad (3)$$

Then,

$$\begin{aligned} \sum_{m=1}^M T_m^I \sin\left(\frac{m\pi}{a}x\right) (F_m^I + B_m^I) &= \\ \sum_{n=1}^N T_n^{II} \sin\left(\frac{n\pi}{a-a_1}(x-a_1)\right) (F_n^{II} + B_n^{II}), & \quad (4) \\ \sum_{m=1}^M T_m^I Y_m^I \sin\left(\frac{m\pi}{a}x\right) (F_m^I - B_m^I) &= \\ \sum_{n=1}^N T_n^{II} Y_n^{II} \sin\left(\frac{n\pi}{a-a_1}(x-a_1)\right) (F_n^{II} - B_n^{II}), & \quad (5) \end{aligned}$$

where F_m and B_m are the amplitudes of incident and reflected waves respectively. T_i are the power normalization terms. L_E and L_H (the report between

input and output field component) can be calculated by power normalization and some algebraic calculation [15]:

$$F^I + B^I = L_E (F^{II} + B^{II}), \quad (6)$$

$$L_H (F^I - B^I) = F^{II} - B^{II}. \quad (7)$$

The S matrix expresses the scattered waves as a function of incident waves:

$$\begin{bmatrix} B^I \\ F^{II} \end{bmatrix} = [S] \begin{bmatrix} F^I \\ B^{II} \end{bmatrix}. \quad (8)$$

From Equations (4) and (5), and to simplify the S matrix calculation, we write it as a vectorioel product:

$$[S] = \text{inv} \begin{bmatrix} I & -L_E \\ -L_H & -I \end{bmatrix} * \begin{bmatrix} -I & L_E \\ -L_H & -I \end{bmatrix}. \quad (9)$$

To check the proper functioning of this analysis, we applied it on a filter already proposed in the literature, and then compare the results.

We chose the filter proposed by Chen in [16], because, as shown in Fig. 4, only resonants irises are used; and this kind of iris necessitates a TE-TM fullwave analysis. Figure 5 shows that the results were very satisfactory.

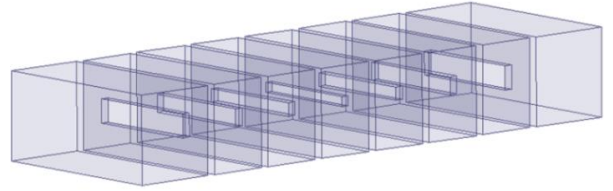


Fig. 4. Seven-iris bandpass filter proposed in [16].

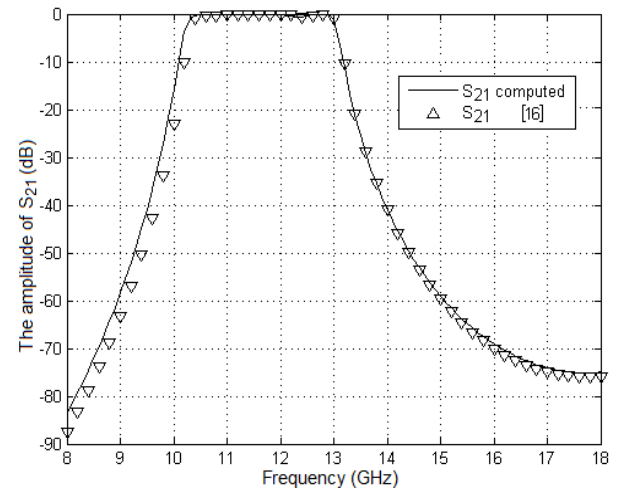


Fig. 5. Frequency response of the seven-iris bandpass filter.

A. Waveguide bend

Considering a waveguide bend in Fig. 6, we can

divide it into three regions, waveguide I, waveguide II, and resonator region III (the center square with the post bounded by the conducting wall, broken line in figure).

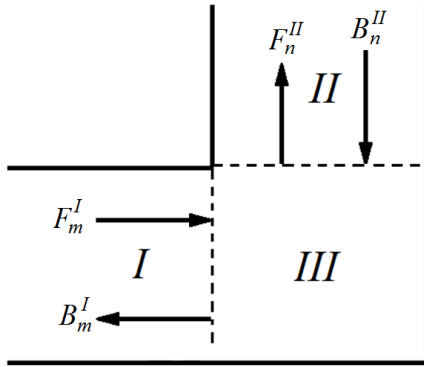


Fig. 6. Waveguide 90° bend.

By an application of a superposition principle, the total fields in the resonator region can be superposed by the field solutions satisfying boundary conditions. Then the fields in this resonator region are derived from the component of the electric and magnetic vector potentials A^i , where F and B , are the unknown eigenmode amplitude coefficients [17]:

$$A^I = \sum_{m=1}^M T_m^I \sin\left(\frac{m\pi}{a} x\right) \left(F_m^I e^{-jk_m^I z} - B_m^I e^{+jk_m^I z} \right), \quad (10)$$

$$A^{II} = \sum_{n=1}^N T_n^{II} \sin\left(\frac{n\pi}{a} z\right) \cdot \left(F_n^{II} e^{-jk_n^{II}(x-a)} - B_n^{II} e^{+jk_n^{II}(x-a)} \right), \quad (11)$$

$$A^{III} = \sum_{m=1}^M C_m^I \sin\left(\frac{m\pi}{a} x\right) \sin(k_m^I(z-a)) + \sum_{n=1}^N C_n^{II} \sin\left(\frac{n\pi}{a} z\right) \sin(k_n^{II} x). \quad (12)$$

Matching the transverse field components at the discontinuities:

$$F^I + B^I = D^I (F^I - B^I) + L^I (F^{II} - B^{II}), \quad (13)$$

$$F^{II} + B^{II} = L^{II} (F^I - B^I) + D^{II} (F^{II} - B^{II}). \quad (14)$$

And then,

$$[S] = inv \begin{bmatrix} I + D^I & -L^I \\ L^{II} & I - D^{II} \end{bmatrix} * \begin{bmatrix} D^I - I & -L^{II} \\ L^I & -D^I - I \end{bmatrix}. \quad (15)$$

Two distinct waveguide bends can be identified, left bend and right bend. Therefore, when the structure contains these two waveguide bends, the bend sense must be taken into consideration. The following examples illustrate the two possibilities; the first, shown

in Fig. 7, is a succession of two bends from different kind, and the second, in Fig. 9, is a succession of two bends from the same kind. Each structure is followed by the comparison of the computed S-parameters and HFSS simulator results. They are shown in Fig. 8 and Fig. 10 respectively, and a good agreement is observed from the curves. In these examples, we used WR75 standard waveguide.

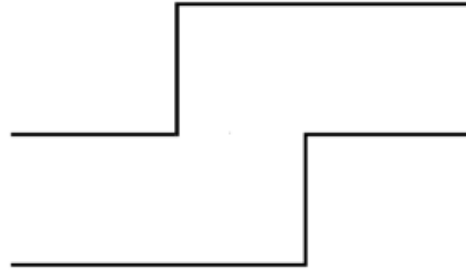


Fig. 7. Succession of two bends from different kind.

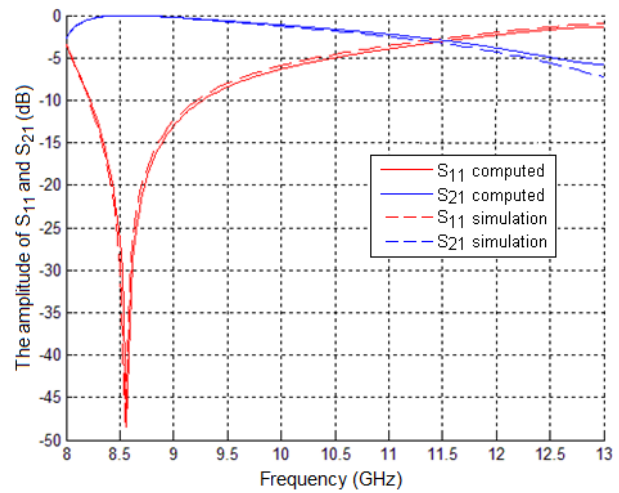


Fig. 8. Computed (—) and HFSS simulated (----) frequency responses of the two bends from different kind.



Fig. 9. Succession of two bends from the same kind.

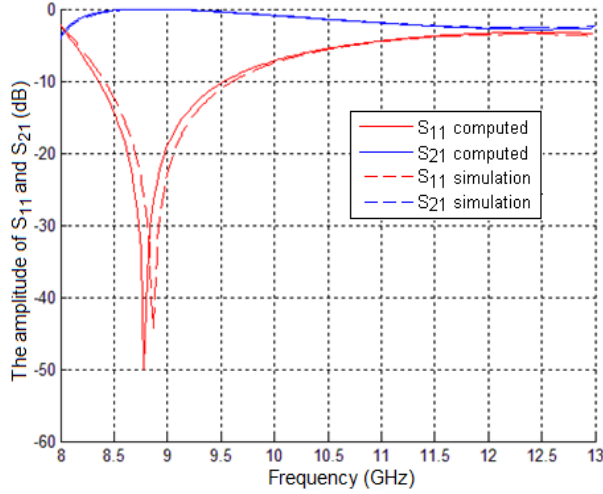


Fig. 10. Computed (—) and HFSS simulated (----) frequency responses of the two bends from same kind.

B. T-junction

To analyze the T-junction, we used the same technique as waveguide bend with adding a third port, then the resonator region becomes formed by three conducting walls (broken line in Fig. 11).

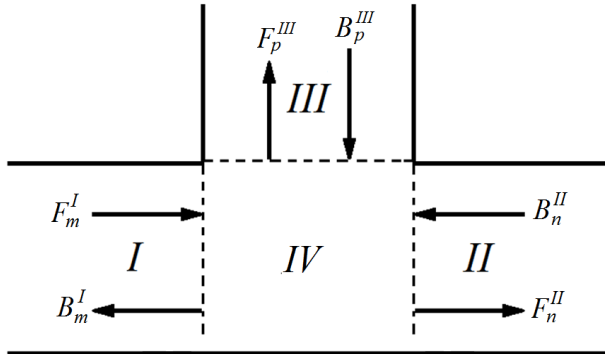


Fig. 11. T-junction.

Vector potentials at the four regions:

$$A^I = \sum_{m=1}^M T_m^I \sin\left(\frac{m\pi}{a} x\right) \left(F_m^I e^{-jk_m^I z} - B_m^I e^{+jk_m^I z} \right), \quad (16)$$

$$A^{II} = \sum_{n=1}^N T_n^{II} \sin\left(\frac{n\pi}{a} x\right) \cdot \left(F_n^{II} e^{-jk_n^{II}(z-a)} - B_n^{II} e^{+jk_n^{II}(z-a)} \right), \quad (17)$$

$$A^{III} = \sum_{p=1}^P T_p^{III} \sin\left(\frac{p\pi}{a} z\right) \cdot \left(F_p^{III} e^{-jk_p^{III}(x-a)} - B_p^{III} e^{+jk_p^{III}(x-a)} \right), \quad (18)$$

$$A^{IV} = \sum_{m=1}^M C_m^I \sin\left(\frac{m\pi}{a} x\right) \sin(k_m^I(z-a)) + \sum_{n=1}^N C_n^{II} \sin\left(\frac{n\pi}{a} x\right) \sin(k_n^{II} z) + \sum_{p=1}^P C_p^{III} \sin\left(\frac{p\pi}{a} z\right) \sin(k_p^{III} x). \quad (19)$$

Matching the transverse field components at the discontinuities:

$$F^I + B^I = D^I (F^I - B^I) + L^{I,II} (F^{II} - B^{II}) + L^{I,II} (F^{II} - B^{II}) + L^{I,III} (F^{III} - B^{III}), \quad (20)$$

$$F^{II} + B^{II} = L^{II,I} (F^I - B^I) + D^{II} (F^{II} - B^{II}) + L^{II,III} (F^{III} - B^{III}), \quad (21)$$

$$F^{III} + B^{III} = L^{III,I} (F^I - B^I) + L^{III,II} (F^{II} - B^{II}) + D^{III} (F^{III} - B^{III}). \quad (22)$$

As for the junction and the bend, we could write the S matrix for the T-junction under the vector product to simplify calculations; the latter will be of great help for the simulation of a complex structure:

$$[S] = \text{inv} \begin{bmatrix} I + D^I & -L^{I,II} & -L^{I,III} \\ L^{II,I} & I - D^{II} & -L^{II,III} \\ -L^{III,I} & -L^{III,II} & I - D^{III} \end{bmatrix} * \begin{bmatrix} D^I - I & -L^{I,II} & -L^{I,III} \\ L^{II,I} & -D^{II} - I & -L^{II,III} \\ -L^{III,I} & -L^{III,II} & -I - D^{III} \end{bmatrix}. \quad (23)$$

For a WR75 waveguide T-junctions, we can note in Fig. 12 a perfect superposition between mode matching analysis and results in [18].

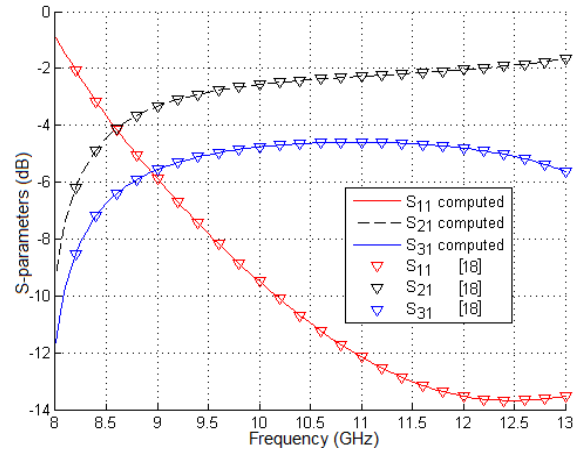


Fig. 12. Frequency response of a WR75 waveguide T-junction.

V. PRACTICAL SWARM OPTIMIZATION PSO

Presented in 1995 by Kennedy, Particle Swarm Optimization (PSO) is a quite recent optimization technique [13]. Like genetic algorithms, it is inspired from nature, so it consists of finding the optimal solution by simulating such social behavior of groups as a bird or bee flocking. It is a simple concept implemented in a few lines of computer code.

Compared to GA, the two methods are favorable to perform with high success rate the tasks of synthesizing microwave structures, with a slight advantage for the GA, but a big advantage for PSO in speed of executing time.

In what follows, we will give the notation and the algorithm of the method.

A. PSO notation

For each particle i :

- x_i is a vector denoting its position and y_i denotes its objective function value.
- y_i is the vector denoting its velocity.
- p_i is the best position that it has found so far and $Pbest_i$ denotes its objective function score.
- g_i is the best position that has been found so far in its neighborhood and $Gbest_i$ denotes the objective function value of g_i .

Velocity update:

- $\vec{U}(0, \varphi_1)$ is a random vector uniformly distributed in $[0, \varphi_1]$ generated at each generation for each particle.
- φ_1 and φ_2 are the acceleration coefficients determining the scale of the forces in the direction of p_i and g_i .
- \otimes denotes the element-wise multiplication operator.

B. PSO algorithm

- Randomly initialize particle positions and velocities.
- While not terminate.
- For each particle i :
 1. Evaluate fitness y_i at current position x_i .
 2. If y_i is better than $Pbest_i$ then update $Pbest_i$ and p_i .
 3. If y_i is better than $Gbest_i$ then update $Gbest_i$ and g_i .
 4. Update velocity y_i and position x_i using:

$$\vec{v}_{i+1} \leftarrow \vec{v}_i + \vec{U}(0, \varphi_1) \otimes (\vec{p}_i - \vec{x}_i) + \vec{U}(0, \varphi_2) \otimes (\vec{g}_i - \vec{x}_i), \quad (24)$$

$$\vec{x}_{i+1} \leftarrow \vec{x}_i + \vec{v}_i, \quad (25)$$

C. Fitness function

The fitness function is an important part of any optimization method; it should evaluate how good the solution is, then the optimal solution is the one which minimizes the fitness function [19]. In this work, we used Discrete Target Approximation [20], which is a simple evaluation of the specifications fulfillment. It consists of assigning to each one of the N frequency points a value of 0 if the response function does not satisfy the corresponding specification, and on the contrary, a value of 1 if it satisfies the specification. The final fitness is the sum of the $\{0,1\}$ values for all the response points, divided by the number of points.

VI. EXAMPLE OF FILTER SYNTHESIS

We applied our combination for the synthesis of a fourth-order waveguide filter. Figure 13 shows the rectangular waveguide filter configuration used in order to implement the matrix (1) into waveguide filter. As mentioned before, the inverters are realized by inserting capacitive or inductive irises depending on the sign of the coupling coefficient in the coupling matrix (inductive iris for the positive coefficient and capacitive iris for negative coefficient) and the resonators are implemented by half-wave resonant cavities, chosen to make the fundamental mode resonate. We aimed to use a side by side waveguide configuration and purely inductive or capacitive irises to facilitate the further manufacturing of filter, using a CNC milling machine. The filter has a central frequency of 10 GHz, a bandwidth of 300 MHz and 20 dB of return loss level. The housing waveguide is a WR75.

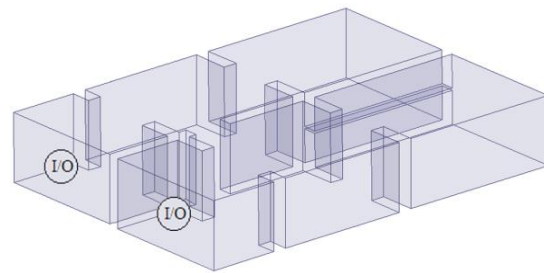


Fig. 13. Geometry of the proposed four-cavity filter.

To analyze the proposed structure, we used the segmentation method [21], which consists of fragmenting the structure into basic elements (seen in the first part of the paper), representing this same structure under network form and then using multi-port networks analysis [22], to analyze the obtained network (Fig. 14), where all the matrices of each segment are put together in a single matrix S_p in Equation (27) [23].

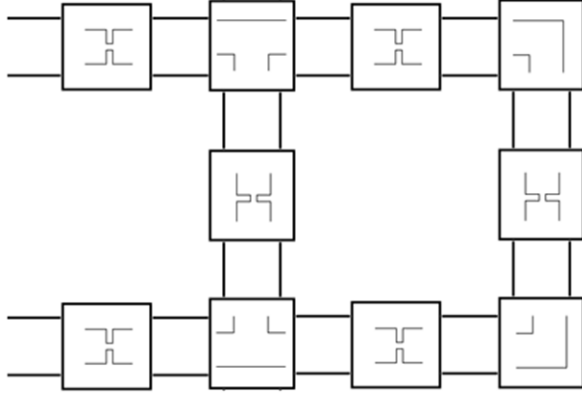


Fig. 14. Structure segmentation for network analysis.

If \bar{a}_p , \bar{b}_p and \bar{a}_c , \bar{b}_c are incident and reflected wave variables at the p external and c internal connected ports. The S_p matrix relating the external port is:

$$\begin{bmatrix} \bar{b}_p \\ \bar{b}_c \end{bmatrix} = \begin{bmatrix} S_{pp} & S_{pc} \\ S_{cp} & S_{cc} \end{bmatrix} \begin{bmatrix} \bar{a}_p \\ \bar{a}_c \end{bmatrix}, \quad (26)$$

$$S_p = S_{pp} + S_{pc}(\Gamma - S_{cc})^{-1}S_{cp}, \quad (27)$$

Γ is the connection matrix that relates adjacent internal ports.

As for the analysis of basic structures and to be assured of the analysis accuracy, we found it necessary to analyze a multi-cell structure treated before and having some similarities with that proposed in this work. We chose the proposed structure in [24] (Fig. 15) where, in both structures, rectangular waveguides are used and the both can be segmented into the same basic elements (junctions, bends and T-junction). The difference is that in the reference filter, the input and output waveguides are superposed, and resonant irises are used. A good agreement is observed in Fig. 16, by comparing the results of multi-port networks analysis and measurement from reference [24].

After the optimization, the finale filter dimensions are illustrated with dimensioning letters in Fig. 17, where the housing waveguide is a standard WR75 (19.0500 mm x 9.5250 mm). The first iris opening (between I/O and cavity ①) is ($a_2=11.5833$ mm) with a shift to the left by ($x_1=3.2430$ mm). The second iris opening (between cavity ① and cavity ②) is ($a_3=8.3379$ mm). The capacitive iris opening (between cavity ② and cavity ③) is ($b_2=0.3000$ mm). The fourth iris opening (between cavity ① and cavity ④) is ($a_4=5.9782$ mm) with a shift to the ports side by ($x_4=0.9809$ mm). The length of the first cavity is ($T=19.0990$ mm) and the length of the second is ($L=23.5963$ mm). The thickness of all irises is 2 mm.

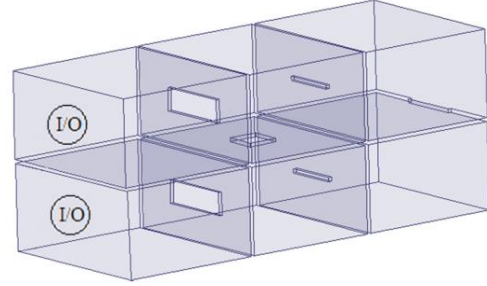


Fig. 15. Configuration of the reference filter [24].

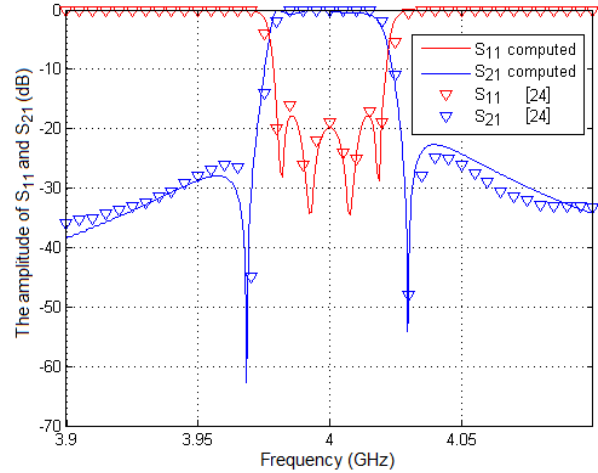


Fig. 16. S-parameters response of the reference filter shown in Fig. 15.

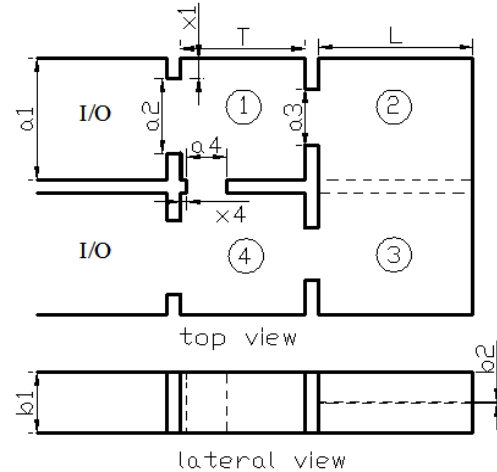


Fig. 17. Filter illustration with dimensioning letters.

Figure 18 shows the comparison between optimized waveguide filter response and equivalent circuit response. We can observe a good fulfillment of the filter specifications, aside from a slight shift of the

right transmission zero.

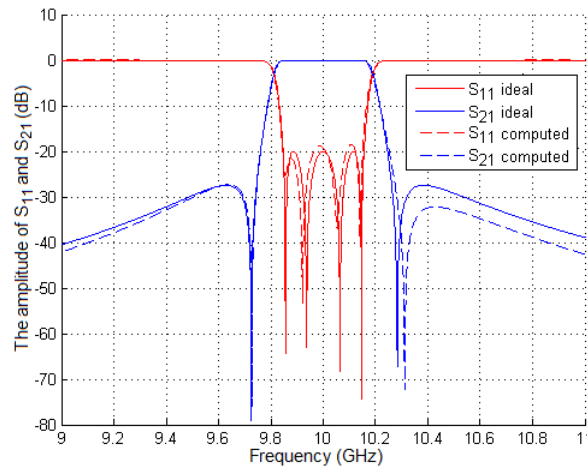


Fig. 18. Ideal circuit response of prototype filter and fullwave computed response.

VII. CONCLUSION

The hardest in the design of microwave filter is to convert a coupling matrix or an equivalent circuit into a microwave structure, this regardless of the manufacturing technique (waveguide, microstrip ... etc.).

This work presents a method for waveguide filter synthesis from predetermined specification. For this, we used a procedure that consists of a series of techniques and methods of calculation, simulation and optimization. All these steps are programmed under Matlab and successfully applied to synthesis waveguide filters.

The direct design by optimization of higher order waveguide filter, without calculating the initial dimensions often tends to fail. This is due to the high number of variables (dimensions of the microwave structure) and also to the high sensitivity of the filter response at very small variation in its dimensions. To alleviate this problem, it is necessary either to divide the structure into several sub-structures, and optimize each one separately, or by calculates the initial dimensions using appropriate approach methods.

REFERENCES

- [1] R. Levy and S. B Cohn, "A history of microwave filter research, design, and development," *IEEE Transactions on Microwave Theory and Techniques*, MTT-32, no. 9, September 1984.
- [2] A. E. Atia, A. E. Williams, and R. W. Newcomb, "Narrow-band multiple-coupled cavity synthesis," *IEEE Transaction on Circuit and Systems*, vol. CAS-21, no. 5, September 1974.
- [3] G. L. Matthaei, L. Young, and E. M. T Jones, *Microwave Filters, Impedance-Matching Networks, and Coupling Structures*. Artech House 1980.
- [4] J. D Rhodes, "The generalized direct-coupled cavity linear phase filter," *IEEE*, MTT-18, no. 6, June 1970.
- [5] A. E Atia and Williams, "Narrow-bandpass waveguide filters," *IEEE Transactions on Microwave Theory and Techniques*, MTT-20, no. 4, pp. 258-265, 1972.
- [6] R. J. Cameron, C. M. Kudsia, and R. R. Mansour, *Microwave Filters for Communication Systems*. John Wiley & Sons, Inc., 2007.
- [7] M. Guglielmi, P. Jarry, E. Kerherve, O. Roquebrun, and D. Schmitt, "A new family of all-inductive dual-mode filters," *IEEE Transactions on Microwave Theory and Techniques*, MTT-49, no. 10, pp 1764-1769, 2001.
- [8] M. Bekheit, S. Amari, and F. Seyfert, "A new approach to canonical dual-mode cavity filter design," *IEEE Transactions on Microwave Theory and Techniques*, vol. 57, no. 5, pp 1196-1206, May 2009.
- [9] M. Guglielmi and C. Newport, "Multimode equivalent network representation of inductive discontinuities," *IEEE Transactions on Microwave Theory and Techniques*, MTT-38, no. 11, pp. 1651-1659, November 1990.
- [10] R. F. Harrington, *Field Computation by Moment Methods*. Wiley-IEEE Press, April 1993.
- [11] R. C Booton, Jr., *Computational Methods for Electromagnetics and Microwaves*. John Wiley & Sons, Inc., Publication 1992.
- [12] H. Patzelt and F. Arndt, "Double-plane steps in rectangular waveguides and their application for transformers, irises, and filters," *IEEE Transactions on Microwave Theory and Techniques*, MTT-30, no. 5, pp. 771-776, May 1982.
- [13] J. Kennedy and R. Eberhart, "Particle swarm optimization," *IEEE*, pp. 1942-1948, 1995.
- [14] N. Marcuvitz, *Waveguide Handbook*. Polytechnic Institute of New Work, December 1986.
- [15] J. Bornemann and R. Vahldieck, "Characterization of a class of waveguide discontinuities using a modified TE_{mn}^x mode approach," *IEEE Transactions on Microwave Theory and Techniques*, vol. 38, no. 12, pp. 1816-1822, December 1990.
- [16] T. S. Chen, "Characteristics of waveguide resonant iris filters," *IEEE Transactions on Microwave Theory and Techniques*, vol. 15, no. 4, pp. 260-262, April 1967.
- [17] T. Sieverding and F. Amdt, "Field theoretic CAD of open or aperture matched T-junction coupled rectangular waveguide structures," *IEEE Transactions on Microwave Theory and Techniques*, vol. 40, no. 2, pp. 353-362, February 1992.
- [18] R. H. MacPhie and K.-L. Wu, "A full-wave

- modal analysis of arbitrarily shaped waveguide discontinuities using the finite plane-wave series expansion," *IEEE Transactions on Microwave Theory and Techniques*, vol. 47, no. 2, pp. 232-237, February 1999.
- [19] J. W. Bandler, "Optimization methods for computation-aided design," *IEEE Transactions on Microwave Theory and Techniques*, vol. 17, no. 8, pp. 533-552, August 1969.
- [20] M. F. J. Nogales, J. P. Garcia, J. Hinojosa, and A. A. Melcon, "Genetic algorithms applied to microwave filters optimization and design," *Progress in Electromagnetics Research Symposium*, Cambridge, USA, pp. 99-103, July 2008.
- [21] T. Okoshi, Y. Uehara, and T. Takeuchi, "The segmentation method—An approach to the analysis of microwave planar circuits," *IEEE Transactions on Microwave Theory and Techniques*, October 1976.
- [22] V. A. Monaco and P. Tiberio, "Computer-aided analysis of microwave circuits," *IEEE Transactions on Microwave Theory and Techniques*, vol. 22, no. 3, pp. 249-263, March 1974.
- [23] R. Chad, and K. C. Gupta, "Segmentation method using impedance matrices for analysis of planar microwave circuits," *IEEE Transactions on Microwave Theory and Techniques*, vol. 29, no. 1, pp. 71-74, January 1981.
- [24] T. Shen, H. T Hsu, K. A. Zaki, A. E. Atia, and T. G. Dolan, "Full-wave design of canonical waveguide filters by optimization," *IEEE Transactions on Microwave Theory and Techniques*, vol. 51, no. 2, pp. 533-552, February 2003.